# Optical- and x-ray-scattering studies of ionic ferrofluids of $MnFe_2O_4$, $\gamma$-$Fe_2O_3$, and $CoFe_2O_4$

M. F. da Silva and A. M. Figueiredo Neto
*Instituto de Física, Universidade de São Paulo, Caixa Postal 20516, 01452-990 São Paulo, São Paulo, Brazil*
(Received 7 May 1993)

Ionic ferrofluids of $MnFe_2O_4$, $\gamma$-$Fe_2O_3$, and $CoFe_2O_4$ has been investigated by means of optical- and x-ray-scattering techniques. The optical birefringence measured as a function of temperature, without any magnetic field, showed the existence of a nematic-type order in these materials. Scattering results indicate the existence of bundlelike aggregates in Mn samples. The origin of the birefringence is discussed in terms of the shape anisotropy of the magnetic particles.

PACS number(s): 61.30.−v, 61.10.Lx, 75.50.Mm, 78.20.Fm

## I. INTRODUCTION

Ferrofluids [1] are colloidal suspensions of small magnetic particles (typical dimensions of 100 Å), dispersed in a liquid carrier. They are fluids like isotropic liquids and have a high magnetic susceptibility. These properties lead to numerous industrial applications such as rotating seals, loudspeakers, and so on [1,2].

Conventional ferrofluids are usually nonaqueous and the classical manufacturing procedures are very long: nanoparticles of magnetic oxide are obtained by grinding and after that the grains are coated with surfactant agents to obtain a suspension in an organic solvent. These ferrofluids were extensively studied by means of scattering techniques [3,4]. The studies indicate that for dillute colloids, the grains look isolated or associated in dimers (or trimers, etc.) depending on the ferrofluid's nature. At higher concentrations, a short-range order appears in the spatial distribution of the grains, even without the magnetic field. The bumps in the x-ray-scattering curves [4] are similar to those of a gas, near its condensation point, or a liquid [5]. The scattering curves indicate the existence of an average distance between first neighbors $\overline{D}$ which decreases for increasing concentration. The grains are distributed in an isotropic way over a sphere of radius $\overline{D}/2$. A paracrystal model [4] was used to explain the experimental results. The reasonable agreement between the experiment and the theoretical calculations indicates that the grains fill all the available space as a gas with interparticle distances that vary with the cubic root of the concentration. The application of a magnetic field, however, can generate elongated aggregates of grains, with the long axis parallel to the field. However, without the magnetic field, the scattering curves are typical of an isotropic fluid.

In 1980, a new mechanism of ferrofluid manufacturing was proposed [6]: colloidal magnetite particles are synthesized by alkaline condensation of Fe ions and, after being electrically charged, are dispersed in an aqueous solution. More recently, ferrofluids of Mn and Co ferrite have been obtained [7] through this new mechanism. Small-angle neutron scattering measurements, performed [8] in ionic ferrofluids of maghemite, gave the radius of gyration of particles as well as their molar mass, in full agreement with magnetization measurements. In a very dilute regime, scattering is typical of isolated particles. In an intermediate concentration (volume fraction of particle $\phi \sim 10\%$), the interparticle interactions can be described [8] considering a second virial coefficient of the osmotic pressure. In this study, the sample was not submitted to a magnetic field.

It is well known that ferrofluids became optically anisotropic [9] when subjected to a magnetic field. This field-induced birefringence could occur due to either the orientation of small aggregates of the magnetic grains or the secondary aggregation of large aggregates into strings. In the absence of field, these superstructures disappear and the fluid remains isotropic.

Recently, results [10] obtained from an ionic ferrofluid of $MnFe_2O_4$ through optical and x-ray scattering have shown the existence of a possible liquid-crystalline nematic-type order. In contrast with the usual ferrofluids, optical and structural characteristics of ionic ferrofluids (in particular those of Mn and Co) were not extensively studied and reported in the literature.

In this paper we report optical-scattering and small-angle x-ray-scattering measurements performed in the ionic ferrofluids of $MnFe_2O_4$, $CoFe_2O_4$ and $\gamma$-$Fe_2O_3$. We also discuss the effect of the magnetic field and temperature upon these ferrofluids. The existence of birefringence without the application of a magnetic field is reported and its possible origin is also discussed.

## II. EXPERIMENT

The ionic ferrofluids studied are composed of $MnFe_2O_4$, $CoFe_2O_4$ and $\gamma$-$Fe_2O_3$ (maghemite-spinel-structure ferric oxide) particles in water, synthesized at Université Pierre et Marie Curie–Paris (France). In Table I we give the characteristics of each sample. The mean diameter of particles ($D_0^{RX}$) were obtained [7] by x-ray-diffraction powder diagrams. Acid samples are composed of magnetic particles positively charged (with $H^+$ at the surfaces) and basic samples have negatively charged particles (with $O^-$ at the surface). The $MnFe_2O_4$ oxides have a spinel-type structure. The elementary cu-

 

TABLE I. Characteristics of the samples studied: $c$ is the concentration of magnetic grains in the sample, $\phi$ is the volume fraction of magnetic material in the solution, and $D_0^{RX}$ is the mean diameter of the particles obtained by the x-ray-diffraction-powder technique. The acids and basic samples are indicated by $A$ and $B$, respectively, in the first column.

| Sample | Particle | Concentration ($c$) ($10^{16}$ grains/cm$^3$) | Volume fraction ($\phi$) (%) | Mean diameter ($D_0^{RX}$) (Å) |
|---|---|---|---|---|
| *S1B* | $\gamma$-$Fe_2O_3$ | 2.2 | 1.30 | 104 |
| *S2B* | $\gamma$-$Fe_2O_3$ | 2.5 | 1.47 | 104 |
| *S3B* | $\gamma$-$Fe_2O_3$ | 3.0 | 1.77 | 104 |
| *S4B* | $\gamma$-$Fe_2O_3$ | 5.0 | 2.8 | 104 |
| *S5B* | $\gamma$-$Fe_2O_3$ | 10.0 | 5.6 | 104 |
| *S6A* | $\gamma$-$Fe_2O_3$ | 5.2 | 2.9 | 104 |
| *S7B* | $MnFe_2O_4$ | 0.5 | 0.06 | 60 |
| *S8B* | $MnFe_2O_4$ | 1.5 | 0.17 | 60 |
| *S9B* | $MnFe_2O_4$ | 2.7 | 0.31 | 60 |
| *S10B* | $MnFe_2O_4$ | 4.0 | 0.46 | 60 |
| *S11B* | $MnFe_2O_4$ | 13 | 1.5 | 60 |
| *S12A* | $CoFe_2O_4$ | 0.5 | 0.99 | 156 |

bic cell is composed of 32 atoms of O, with 64 interstices of tetrahedral symmetry and 32 of octahedral symmetry, where the Mn ions are placed.

Before each experiment, the ferrofluid's quality is carefully verified. A sample of ferrofluid is used in a laser scattering experiment in order to verify the existence of large clusters (dimensions of about 1 $\mu$m). Only samples that do not present light scattering are used in the optical and x-ray experiments.

### A. Optical experiment

The sample was encapsulated in microslides (thickness $d=50$, 100, 200, and 400 $\mu$m), (width 2.5, 5 mm and length 20 mm). Then the ferrofluid was put inside the microslide by flux. Both extremities of the microslide were melted to avoid evaporation of water. During the sealing process special care was taken to avoid the heating of the ferrofluid inside the microslide. The sample's temperature was controlled to within 0.01 K (Instec HS 1-i hot stage). The observations were made in an orthoplan polarized (Leitz) microscope with a tilting compensator to measure the birefringence. Care was taken to avoid spurious external fields in the sample, since ferrofluids are sensitive to small magnetic fields. It was also used a microscope plate, made of a nonmagnetic material.

We also studied the birefringence induced by a magnetic field $H$ in the sample. The experimental setup comprised a temperature-controlled device (stability of 0.5 °C) in which the sample (microslide) was placed, and a magnetic field of controlled strength ($3<H<1500$ G) was applied to the sample.

The laboratory frame was defined as follows: the $z$ axis was perpendicular to the largest surface of the microslide (light's propagation direction); the $x$ axis was parallel to the microslide length and $y$ was the third orthogonal axis.

### B. X-ray-scattering experiment

The x-ray-scattering experiment was carried out in the synchrotron at the Laboratoire pour l'Utilisation du Rayonnement Electromagnetique (LURE) in Orsay, France [small-angle x-ray scattering (SAXS), D24 station].

The samples were sealed in Lindemann glass capillaries (0.5 mm diameter). They were placed in a temperature-controlled device (accuracy $\pm 0.3$ °C), and irradiated by x-ray monochromatic radiation [Ge(111) crystal, wavelength $\lambda=1.608$ Å]. The SAXS curves were registered in a *linear detector sensitive to the position,* connected to a VAX station where the data analysis was done. The distance from the sample to the detector was 1646 mm. Each SAXS curve is composed by mean values of four independent spectra, each obtained during an aquisition time of 100 sec.

The laboratory frame is defined as follows: the $z$ axis was parallel to the capillary axis (horizontal direction); the $x$ axis was parallel to the x-ray beam, and $y$ was the third orthogonal axis (vertical direction). The linear detector could be placed in both the vertical and horizontal directions.

## III. RESULTS AND DISCUSSION

### A. Optical results

#### 1. *Birefringence ($\Delta n$) at zero magnetic field*

All the ionic ferrofluids encapsulated in microslides present a small optical birefringence without application of a magnetic field. In all cases, the optical axis of the sample (**n**) orients parallel to the longest axis of the microslide ($x$ axis), i.e., along the filling flux direction. The fact that **n** is oriented along the $x$ axis in all the experiments (for different relative orientations of the microslide in the microscope) clearly confirms that the measured birefringence does not occur due to spurious external fields. The sign of $\Delta n$ ($=n_e-n_o$, where $n_e$ and $n_o$ are the extraordinary and ordinary refractive indices, respectively) is negative for $\gamma$, Co, and Mn samples. The birefringence of the empty microslide $\Delta n_c$ was measured and presented a constant value as a function of the temperature ($T$): $\Delta n_c<-0.7\times10^{-5}$ ($d=200$ $\mu$m).

The measured birefringence is independent of the sample thickness. Typical results are presented (Table II) in the samples $S4B$ and $S12A$ at $T=24\,^{\circ}\mathrm{C}$. Similar results were obtained with the different samples (Table I). These results indicate that the observed birefringence occurs due to the sample's bulk and not only for thin layers, near the microslide glass boundaries.

The typical behavior of $\Delta n$ as a function of $T$ is presented in Fig. 1 (maghemite sample) and Fig. 2 (Mn sample). Each point on the curve is a mean value of several independent measurements (experimental error $\sim 6\%$). In the figures, the crosses represent $\Delta n$ measured for increasing temperatures and the circles for decreasing temperatures. The absolute values of $\Delta n$ of maghemite samples are about three times greater than the value of $\Delta n$ in Mn and Co samples with the same particle's concentration. We will be back to this point later on. The behavior of $\Delta n$ clearly identifies an anisotropic fluid in the temperature ranges investigated. The phenomenon was observed with all the ionic ferrofluid samples investigated. The same optical experiment performed with the commercial water-based ferrofluid $Fe_3O_4$ ($2\times10^{16}$ grains/cm$^3$), coated with oleic acid (Ferrofluidics Corporation) does not show birefringence; the fluid is isotropic in all investigated temperature ranges ($17<T<88\,^{\circ}\mathrm{C}$).

As temperature increases starting from room-temperature ($\sim 20\,^{\circ}\mathrm{C}$), $\Delta n$ of ionic ferrofluid samples increases, reaching a maximum value, and after that it decreases. In particular, with the Mn samples (see Fig. 1 of Ref. [10]), $\Delta n$ goes to zero [10] $T\geq 87.16\,^{\circ}\mathrm{C}$. The jump of $\Delta n$ in the transition to the isotropic phase [10] could not be measured. Optical observations of Mn samples indicate that for $T>89\,^{\circ}\mathrm{C}$ there is a segregation between the magnetic particles and water. After heating the Mn sample ($T_{\max}<89\,^{\circ}\mathrm{C}$), and coming back to lower temperatures, for a waiting period of two hours, $\Delta n$ systematically decreases and does not return to the original value (circles in Fig. 2). The same experiment performed with $\gamma$-$Fe_2O_3$ samples, presents a different behavior. Acid samples ($S6A$) do not present a measurable hysteresis, i.e., going up and down with $T$, $\Delta n$ follows the curve of Fig. 1. If there is a relaxation time of birefringence, it is smaller than temperature stabilization time, evaluated in about 1 min. Basic samples, however $S1B$–$S5B$, presented a different behavior: after heating and coming back to lower temperatures, $\Delta n$ is smaller than the original value but, as a function of time, $\Delta n$ returns to the original value. Figure 3 shows $\Delta n$ at a fixed temperature $T=20\,^{\circ}\mathrm{C}$ (after heating and cooling processes) as a function of time. Fitting an exponential law ($\Delta n=ae^{-t/\tau}+b$), where $a$ and $b$ are constants, the relaxation $\tau$ time can be determined. This parameter presents a dependence on temperature, as shown in Fig. 4: $\tau$ decreases for increasing values of $T$.

### 2. Birefringence ($\Delta n$) with $H\neq 0$

The field-induced birefringence of ferrofluids can be written as [11]

$$\frac{\Delta n}{\Delta n_s}=\frac{\int_0^{\infty} y^2[1-(3\coth\alpha/\alpha)+3/\alpha^2]\exp[-(\ln^2 y/2\sigma^2)]dy}{\int_0^{\infty} y^2\exp[-(\ln^2 y/2\sigma^2)]dy} \tag{1}$$

with $\alpha=AD_0^3y^3H$, $A=\pi m_s/(6k_BT)$, and $y=D/D_0$, where $\Delta n_s$ is the birefringence at saturation, $m_s$ is the saturation magnetization of the material in the grain, $\sigma$ is the standard deviation of $D_0$ which is the grain diameter, $D$ is the mean diameter of the grain distribution, $k_B$ is the Boltzmann's constant, and $T$ is the temperature.

Figures 5(a) and 5(b) show the results of $\Delta n$ and $\Delta n/\Delta n_s$, respectively, measured at $T=23$ and $53\,^{\circ}\mathrm{C}$ with sample $S5B$. Figures 6(a) and 6(b) show $\Delta n$ and $\Delta n/\Delta n_s$, respectively, measured at $T=20$ and $50\,^{\circ}\mathrm{C}$ with the $S7B$ sample as a function of $H$. Similar curves were obtained with other samples (Table I). Indeed, our results of Mn samples [Fig. 6(a)], indicate that for increasing values of $T$, the absolute value of $\Delta n$ increases. In maghemite samples, this effect is not clearly observed [Fig. 5(a)]. The absolute value of $\Delta n_s$ of maghemite samples is about seven

TABLE II. Optical birefringence ($\Delta n$) as a function of the sample thickness ($d$). The experiment's temperature is $T=24\,^{\circ}\mathrm{C}$. [(*) The Co samples, even for low concentrations have low transmittance. In this case, the error in $\Delta n$ is about 12%.]

| Sample | $d$ ($\mu$m) | $-10^5\Delta n$ ($\pm 6\%$) |
|---|---|---|
| $S4B$ | 50 | 3.6 |
| | 100 | 3.9 |
| | 200 | 3.8 |
| | 400 | 3.9 |
| $S12A$ | 50 | 0.3* |
| | 100 | 0.3* |

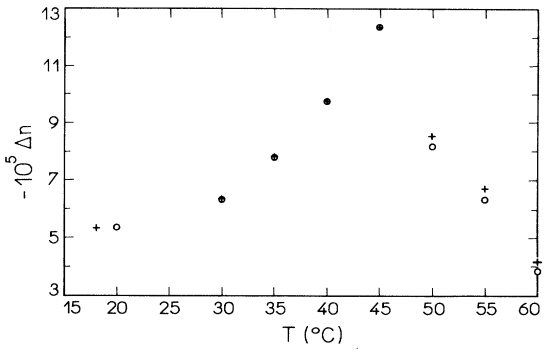


FIG. 1. Optical birefringence $\Delta n$ of $\gamma$-$Fe_2O_3$ as a function of the temperature $T$. Sample $S6A$. (+) increasing temperatures, (○) decreasing temperatures.

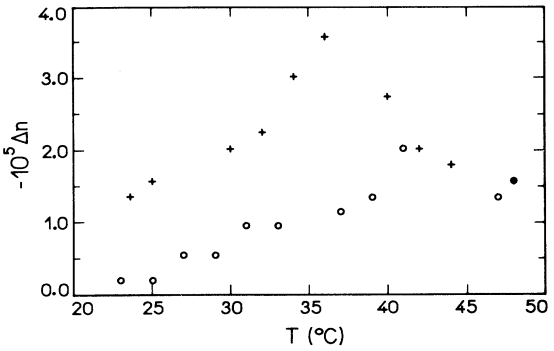


FIG. 2. Optical birefringence $\Delta n$ of $MnFe_2O_4$ as a function of the temperature $T$. Sample $S7B$. (+) increasing temperatures, (○) decreasing temperatures.

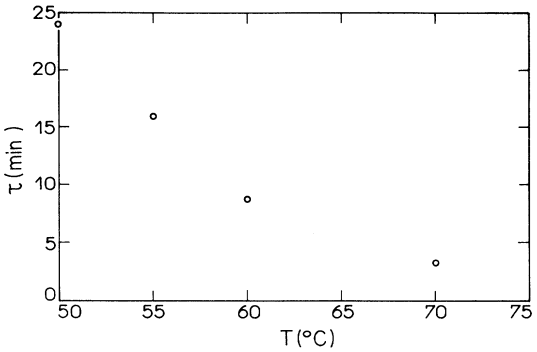


FIG. 4. Relaxation time of $\Delta n$ as a function of the temperature $T$. Sample $S4B$.

times greater than the $\Delta n_s$ values of Mn samples, at the same particle concentration.

Figure 5(b) shows a fit of Eq. (1) to the experimental results of a maghemite samples: $m_s=400$ G, $\sigma=0.2$, $D_0=150$ Å. The quality of the fit indicates that we have a polydisperse sample in terms of the particle's dimensions, not entirely described by a log-normal distribution law [11]. Equation (1), however, can give us an evaluation of $D$. Our results indicate that in maghemite samples there are essentially single particles ($D_0\sim 150$ Å and $D_0^{RX}=104$ Å). Small aggregates (dimers and trimers) could also exist. These optical results were not particularly sensitive to the temperature (Fig. 5).

In Mn samples, as the absolute values of $\Delta n$ versus $H$ are smaller compared with maghemite samples, the effect of the temperature is more visible [Fig. 6(a)]. Figure 6(b) shows the experimental results of $\Delta n/\Delta n_s$ as a function of $H$ and two theoretical curves [Eq. (1)] with: $m_s=200$ G, $\sigma=0.3$, $D_0=200$ Å (dotted line), and $D_0=250$ Å (solid line). As in the case of maghemite samples, a log-normal distribution of $D$ [11] does not seem to reasonably fit the Mn results.

Assuming Eq. (1) as a first-order approach to evaluate $D_0$, we can conclude that even at 20 °C, the Mn sample already has a large number of aggregates of particles. The dotted line in Fig. 6(b) has $D_0=200$ Å and the particle has $D_0^{RX}=60$ Å. At 50 °C, the fit of Eq. (1) to the experimental results indicate the $D_0$ increases to about 250 Å. This small-scale aggregation process as a function of $T$ will be discussed in Sec. IV.

The measured birefringence at saturation depends on the magnetic grain concentration in the sample. Figures 7(a) and 7(b) show $\Delta n_s$ (at $T\sim 20$ °C) as a function of the particle concentration for $\gamma$ and Mn samples, respectively. The results of maghemite samples presented [Fig. 7(a)] indicate that the birefringence is proportional to the

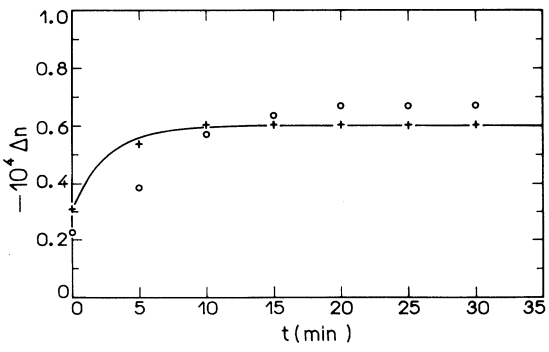


FIG. 3. Time evolution of the birefringence of a basic $\gamma$-$Fe_2O_3$ ionic ferrofluid. Sample $S4B$. $\Delta n$ measured at $T=20$ °C. Sample heated up to (○) 60 °C and (+) 70 °C before the $\Delta n$ measurements. (——) exponential law fit to (+).

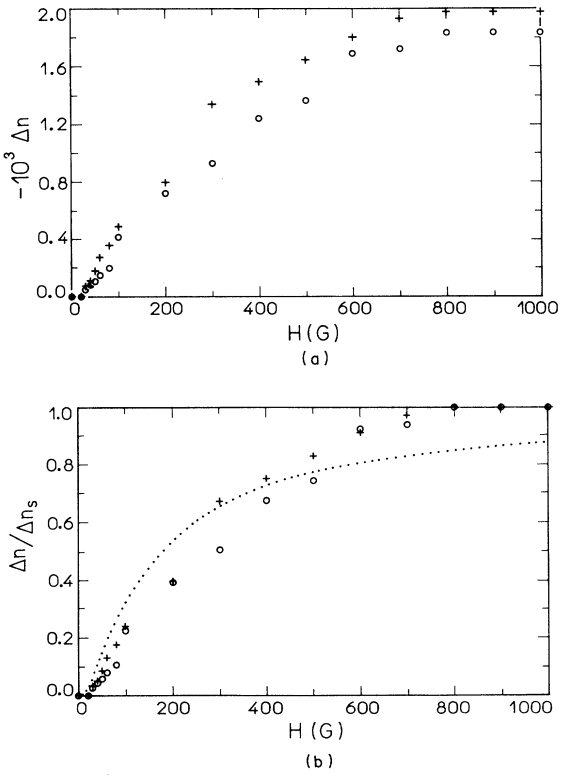


FIG. 5. Sample $S5B$ at $T=23$ °C (○) and 53 °C (+): (a) birefringence $\Delta n$ as a function of $H$; (b) $\Delta n/\Delta n_s$ as a function of $H$. (· · ·) is a theoretical fit using Eq. (1). (See text.)

particle concentrations ($\Delta n \alpha c$). The linear dependence between $\Delta n$ and $c$ was also experimentally found [12] in usual nonionic ferrofluids of Co and $Fe_3O_4$ (organic based) and $Fe_3O_4$ (water based). This behavior, however, does not seem to be universal. Hayes [13] reported measurements of the optical anisotropy of the colloidal $Fe_3O_4$ (magnetite) in which an increase of $10^4$ times the concentration gave only a factor of two on the optical anisotropy. From the theoretical point of view, Scholten [14] analyzed the anisotropic spatial ordering of single particles and found a quadratic law for the optical anisotropy: $\Delta n \alpha c^2$, not experimentally verified. We shall go back to this point later on.

Mn samples [Fig. 7(b)] do not present the same behavior as maghemite samples. A function of the type ($\Delta n \alpha c^{1/2}$) seems to describe the experimental results.

### B. X-ray-scattering results

Small angle x-ray-scattering measurements were performed with *S5B*, *S10B*, and *S11B* samples as a function of temperature and magnetic field (*H* has always been applied perpendicular to the capillary axis).

#### *1. $\gamma$-$Fe_2O_3$ samples*

Figure 8 shows the typical SAXS curves of sample *S5B* along the directions parallel and perpendicular to the capillary axis. Within accuracy in the experiment, we did not observe significant differences between the SAXS curves in temperature and magnetic-field ranges of $20 < T < 60$ °C and $10 < H < 1000$ G. Guinier's plot [5] of the SAXS curves are presented (Fig. 9) for both experimental configurations in the range $0 < s^2$ ($= 4 \sin^2\theta/\lambda^2$,

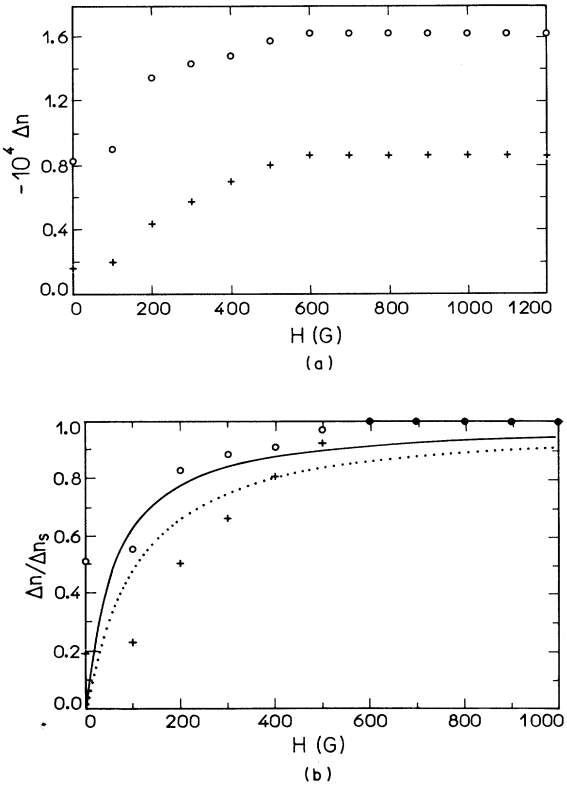


FIG. 6. Sample *S7B* at $T = 20$ °C (+) and 50 °C (○): (a) birefringence $\Delta n$ as a function of $H$; (b) $\Delta n / \Delta n_s$ as a function of $H$. (−) and (· · ·) are theoretical fits using Eq. (1). (See text.)

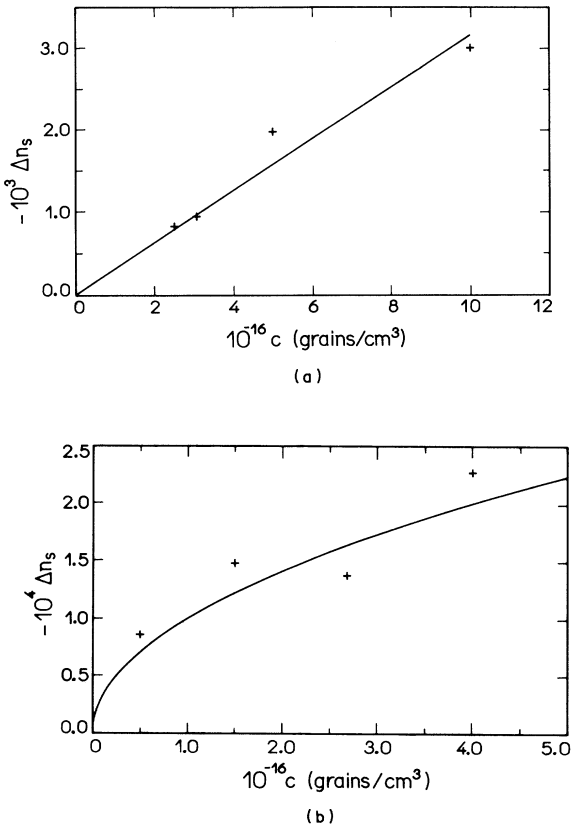


FIG. 7. Birefringence at saturation (at $T = 20$ °C) as a function of the magnetic particle concentration (c) of ionic ferrofluids. (a) $\gamma$-$Fe_2O_3$ samples. The solid line is a linear fit $\Delta n_s = -3.16 \times 10^{-20}$ c. (b) $MnFe_2O_4$ samples. The solid line is a fit of the function $\Delta n_s = -10^{-12} c^{1/2}$.

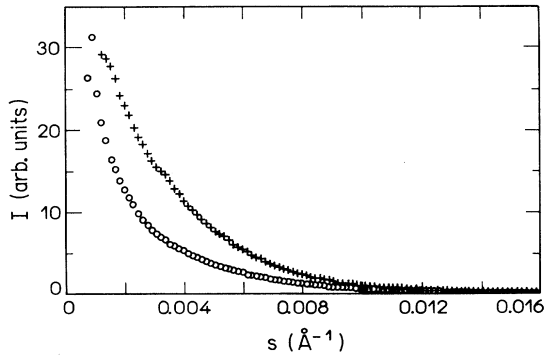


FIG. 8. Small-angle x-ray-scattering curves at $T = 24$ °C and $H = 10$ G. *S5B* (maghemite) sample in a capillary. $I$ is the intensity in arbitrary units and $s$ is the modulus of the scattering vector. (+) scattering parallel to the capillary axis, (○) scattering perpendicular to the capillary axis.

where $\lambda$ is the x-ray wavelength and $2\theta$ is the scattering angle) $<10^{-4}$ Å$^{-2}$. The linear part of the curves $\ln I(s)$ versus $s^2$ [where $I(s)$ is the scattered intensity] is related to the Guinier's radius $R_G$ by the equation [5]

$$\ln I(s) = A - \frac{4\pi^2}{5} R_G^2 s^2 , \quad (2)$$

where $A$ is a constant. Figure 9 presents a linear region in the range $0.3\times10^{-4} < s^2 < 10^{-4}$ Å$^{-2}$. For $s^2 < 0.3\times10^{-4}$ Å$^{-2}$, a rounding off in the curve is observed. The linear part gave $R_G = 54$ Å for both curves. This value is in agreement with the particle dimensions measured by means of independent techniques (the mean diameter is $D_0^{RX} = 104$ Å; see Table I). The rounding off for small values of $s$ indicates that bigger particles are present in the sample. We evaluate that the Guinier's radius of such distributions of particles lies in the intervals $54 < R_G^{\perp} < 100$ Å and $54 < R_G^{\parallel} < 200$ Å along the directions perpendicular and parallel to the capillary axis.

The experimental results indicate that there are small aggregates of particles in the sample. These aggregates are anisometric, being larger along the applied magnetic field direction, i.e., along their total magnetic moment direction. A possible picture of this structure is that there are monomers and dimers in the direction perpendicular to **H** and trimers and tetramers in the direction of **H**. As the rounding off of the SAXS curves is only observed in a small range of $s$, the number of aggregates is expected to be small compared to the one of single particles (monomers).

As the shape of the SAXS curves was not sensitive to variations of $H$ in the range $10 < H < 1000$ G, the aggregates observed do not occur due to the field.

### 2. *$MnFe_2O_4$ samples*

Figures 10(a) and 10(b) show the typical SAXS curves of Mn samples along the directions parallel and perpendicular to the capillary axis, respectively. Within accuracy in the experiment for a given sample concentration, we did not observe significant differences between the SAXS curves in temperature and magnetic-field ranges of $20 < T < 60$ °C and $10 < H < 1000$ G.

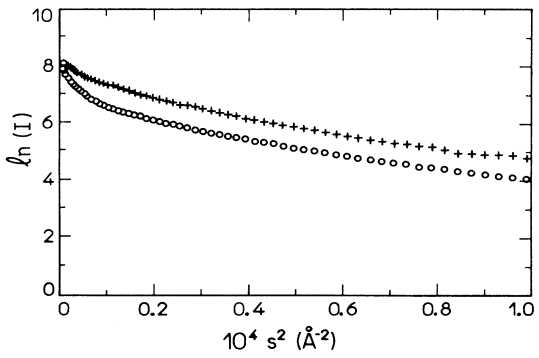


FIG. 9. Guinier's plot of Fig. 8 *S5B* sample. (○) scattering perpendicular to the capillary axis, (+) scattering parallel to the capillary axis.

The SAXS curves of Mn sample [Fig. 10(b)] in both concentrations studied present a bump at $s_1 \sim 2.2\times10^{-2}$ Å$^{-1}$ and a broad band at $s_2 = 3.89\times10^{-2}$ Å$^{-1}$, at the configuration parallel to **H**. The positions of the bump and band were not affected by temperature, magnetic field or sample concentration (*S10B* and *S11B* samples). The SAXS curve intensity in the most concentrated sample (*S11B*) is bigger than the intensity in the diluted sample (*S10B*).

In dense systems, correlations between grains are supposed to appear. In addition to the scattered intensity related to the isolated particles, there are also interparticular interferences. In order to interpret the SAXS curves in such conditions, the paracrystal model [4] is often used. In this model, the particle centers are close to the sites of a distorted compact lattice. The position of the first maximum ($\bar{d}$) is defined by

$$s\bar{d} = 1.22 . \quad (3)$$

In this picture we have

$$\bar{d}_1 \simeq 55 \text{ Å} ,$$

$$\bar{d}_2 \simeq 31 \text{ Å} ,$$

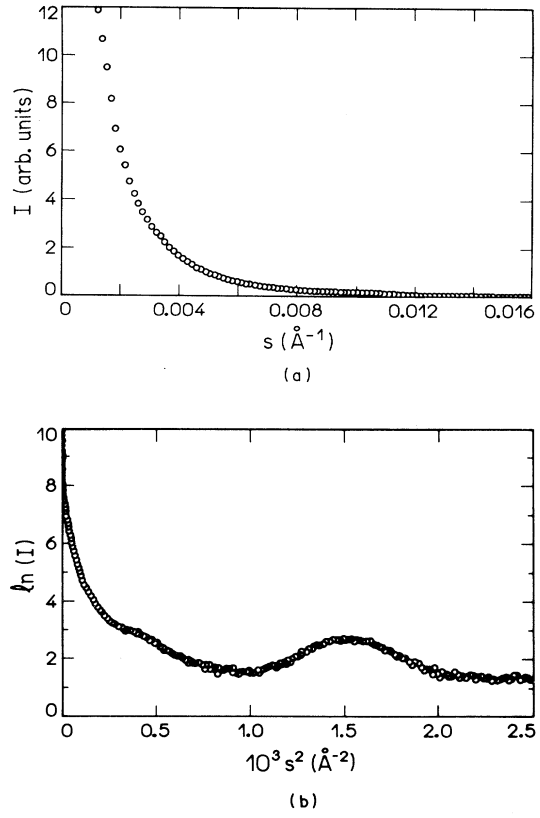


FIG. 10. Small-angle x-ray scattering curves at $T = 24$ °C and $H = 10$ G. *S11B* (Mn) sample in a capillary. $I$ is the intensity in arbitrary units and $s$ is the modulus of the scattering vector: (a) along the direction parallel to the capillary axis; (b) along the direction perpendicular to the capillary axis, $\ln I$ vs $s^2$.

which correspond to $s_1$ and $s_2$, respectively.

The SAXS curves in the configuration perpendicular to **H** [Fig. 10(a)] do not show any structure with bumps or bands. The Guinier's plot of the SAXS curves in this configuration is shown in Fig. 11. A linear region (which follows the Guinier's law) is observed in the range $0.55\times10^{-4}<s^2<10^{-4}$ Å$^{-2}$, corresponding to $R_G^{\perp}\sim56$ Å. Out of this range, Fig. 11 shows a rounding off, which is more accentuated at small angles ($s^2<0.2\times10^{-4}$ Å$^{-2}$). As in the case of the maghemite samples, this result indicates the existence of a size distribution of aggregates of particles in the sample. This distribution seems to be broader in Mn samples than in $\gamma$-$Fe_2O_3$ samples. We evaluate the limits of this distribution in terms of $R_G^{\perp}$ as being $56<R_G^{\perp}<105$ Å.

The mean diameter of Mn particles (see Table I) is about 60 Å. A trial structure we can imagine to explain the experimental results consists of anisometric aggregates of particles in a deformed hexagonal array. These aggregates (needles) are bigger along the magnetic moment direction of particles than in the direction perpendicular to it. The dimensions $\bar{d}_1$ and $\bar{d}_2$ should correspond to the $d_{100}$ and $d_{110}$ crystallographic planes [15], respectively. The ratio between $\bar{d}_1$ and $\bar{d}_2$ is

$$\frac{\bar{d}_1}{\bar{d}_2}\sim1.77\ ,$$

very close to the expected value of the HCP array [15] $\sqrt{3}$. The lattice parameter of this deformed HCP cell is about 62 Å, which is in agreement with $D_0^{RX}$ (Table I). In the direction perpendicular to the particle's magnetic moment, the aggregates are small and there is not enough positional correlation to produce bump or band in the SAXS curves. The evaluation of $R_G^{\perp}$ (made above), indicates that we can have a packing from two to three particles along this direction.

The width at half height of the band ($\Delta s$) and Scherrer's equation [5] can be used to evaluate the dimension of the aggregate of grains ($D^*$) in the direction parallel to its magnetic moment (parallel to **H**):

$$D^*\sim\Delta s^{-1}\ . \tag{4}$$

The width measured in our experiments is $\Delta s_m\simeq7.4\times10^{-3}$ Å$^{-1}$. The experimental broadening $\Delta s_e$ of the setup in our conditions is about $3\times10^{-3}$ Å$^{-1}$.

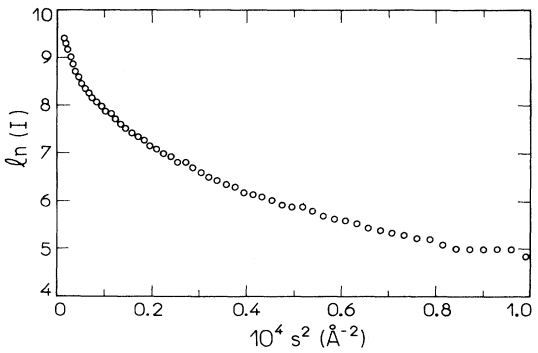


FIG. 11. Guinier's plot of Fig. 10(a) *S*11*B* (Mn) sample. Scattering perpendicular to **H**, parallel to the capillary axis.

The three widths are related by the equation

$$(\Delta s_m)^2=(\Delta s)^2+(\Delta s_e)^2\ . \tag{5}$$

Using Eqs. (4) and (5) we obtain $\Delta s\sim7\times10^{-3}$ Å$^{-1}$ and $D^*\sim150$ Å. Associating the origin of the band with the $d_{110}$ planes, $D^*\sim5d_{110}$. The complete trial structure we can imagine for these aggregates is a bundle consisting of the superposition of three or four linear strings of particles (with their magnetic moment parallel to each other) in a deformed HCP array. This symmetry of the array is necessary to stabilize the magnetic structure. A cubic array, for example, is forbidden for magnetic reasons. This point can be qualitatively verified if we suppose the packing of small (spherical for simplicity) permanent magnets, consider two linear clusters of these magnets with their magnetic moments aligned parallel to each other. The most stable configuration of these two lines in the presence of a magnetic field is that where the linear clusters are parallel to **H**, with the centers of mass of spherical magnets in a hexagonal array. In a simple cubic array, the system would be unstable since two parallel magnets (parallel magnetic moments) feel repulsive forces due to the neighbor.

The existence of these bundles was observed in diluted samples (*S*10*B*) and in more concentrated samples (*S*11*B*) as well. As the SAXS shape was not sensitive to variations of $H$ in the range $10<H<1000$ G, the needles observed are not due to the field. Even after $H$ is switched off, the SAXS curves in both configurations remain unchanged.

## IV. THE ORIGIN OF THE BIREFRINGENCE

The origin of $\Delta n$, even at zero field, is a puzzling question. Two different mechanisms should be taken into account: the crystalline and the shape anisotropy of particles. In particular, as the ionic ferrofluids have a spinel-type (cubic) structure, one would expect no crystalline anisotropy. The existence of defects [16] in this structure could produce this anisotropy. The shape anisotropy shall be discussed in more details.

Consider a prolate-ellipsoidal particle of axes $2a$ and $2b$ ($a>b$), and aspect ratio $c^*=(b/a)=0.939\,69$, which corresponds to a shape anisotropy of about 5%. The depolarizing factors along the long and the short axes are [17]: $A_a=0.316\,90$ and $A_b=0.341\,55$, respectively. The optical anisotropy ($\Delta g$) of this object, due to this anisometry, can be calculated using the equation [18]

$$\Delta g=g_b-g_a=\frac{1}{4\pi}\left\{\frac{n_b^2-n^2}{1+[(n_b/n)^2-1]A_b}-\frac{n_a^2-n^2}{1+[(n_a/n)^2-1]A_a}\right\}, \tag{6}$$

where $n_b$ and $n_a$ are the refractive index of particle by light polarized in the directions parallel to the short and long axes, respectively; $n$ is the refractive index of the solvent. Considering $\gamma$-$Fe_2O_3$ particles in water, one has

$n=1.3$; $n_a=n_b=2.8$ [19]. With these values in Eq. (6), we have

$$\Delta g = g_b - g_a = -9.1\times10^{-3} . \quad (7)$$

The birefringence $\Delta n_s$ can be calculated using the equation [14]

$$\Delta n_s = \frac{2\pi\phi}{n}\Delta g , \quad (8)$$

where $\Delta n_s$ is the birefringence at saturation (all particles aligned parallel to each other).

Two important conclusions can be obtained from Eqs. (7) and (8). The sign of $\Delta g$ (and $\Delta n_s$) is negative for prolate-ellipsoidal particles. It happens because the optical axis is parallel to the longest axis of the ellipsoid and

$$\Delta n = n_e - n_o = n_b - n_a . \quad (9)$$

This sign is in agreement with the measurement performed with ionic ferrofluids in this work. Another important conclusion is that as $\phi$ is proportional to the particle concentration $c$, $\Delta n_s$ is also proportional to $c$. This prediction for Eq. (8) is experimentally observed in our results with maghemite samples [Fig. 7(a)], as discussed above.

The values of $\Delta g$ can be evaluated for each sample from the measurements of $\Delta n_s$.

In maghemite samples (*S6A*, for example), $\Delta n_s=-1.3\times10^{-3}$ at 23 °C and $\Delta n_s=-1.5\times10^{-3}$ at 53 °C. Using these values in Eq. (8) we have $\Delta g=-9\times10^{-3}$ at 23 °C and $\Delta g=-11\times10^{-3}$ at 53 °C, in good agreement with the theoretical value [Eq. (7)].

In Mn samples (*S7B*, for example), $\Delta n_s=-0.87\times10^{-4}$ at 20 °C and $\Delta n_s=-1.6\times10^{-4}$ at 50 °C. Using Eq. (8) we obtain $\Delta g=-30\times10^{-3}$ at 20 °C and $\Delta g=-56\times10^{-3}$ at 50 °C. These values need a more anisometric particle (or an aggregate) to be responsible for the observed birefringence. If we take the anisometry of the bundle-shaped aggregates observed in the SAXS experiment, they have an aspect ratio $c^*\sim0.33$. The value of $\Delta g$ calculated using Eq. (6) is about $-36\times10^{-3}$, in good agreement with the experimental values at room temperature.

As the experimental values of $|\Delta g|$ for both ferrofluids are bigger at about 50 °C compared to the values at 20 °C, a small-scale aggregation that would change the anisometry of the particles a little bit seems to take place. The origin of this aggregation process could be a modification of the chemical equilibrium between the solution and the grains, that keeps their surfaces electrically charged. Since the ferrofluids are produced at room temperature, the equilibrium of the chemical reaction that electrically charges the grains gives a stable colloid of independent particles at about 20 °C. In the case of Mn samples, however, the bundles seem to exist even at a room temperature. The equilibrium should be disturbed with increasing temperatures, so at the surface electric charge decreases and some agglomeration occurs.

In maghemite samples, this process of modification of the surface density of the particles seems to be reversible: acid samples do not present a measurable hysteresis and basic samples present a relaxation time of the order of minutes (Sec. III A 1). In Mn samples, however, the aggregation process seems to be irreversible.

Concerning the birefringence at zero magnetic field measured in all the ionic ferrofluid samples studied in this work, some final remarks could be made. One of the most important differences between these ferrofluids and conventional isotropic ferrofluids is that in our case, the grains have an electric charge. It has been known for a long time that repulsion alone induces nematic order in elongated molecules. An anisotropic charge distribution in the ferrofluid grains could be one of the responsible interactions for the nematic order. In the case of thermotropics, the anisometry of the molecules is usually bigger than the anisometry of the ferrofluid grains or even the bundles. This fact seems to indicate that other mechanisms are needed to explain the nematic order. Two other aspects must be taken into consideration: the role of the polar solvent (water) and the magnetic interactions between the grains. Since water is a polar molecule, one could suspect that the solvent would play an important role in producing this long-range orientational ordering of the grains. It is well known that water plays an important role in physicochemical properties in lyotropic liquid crystals. Each grain has a magnetic moment of $10^{-19}$ A m$^2$ (Mn samples), which is about the same order of magnitude as the magnetic moments of usual ferrofluids (nonionics). Since the nematic order is not observed in usual ferrofluids, the magnetic interaction alone does not seem to be responsible for the appearance of the nematic ordering. It is not possible, at this stage of our knowledge, to elect the most important mechanism that promotes the nematic ordering in ionic ferrofluids. Perhaps all the different mechanisms are important and play a complementary role in order to give this property to ionic ferrofluids. New experiments will be necessary to clarify these points.

## V. CONCLUSIONS

The optical and x-ray results obtained with the ionic ferrofluids $MnFe_2O_4$, $\gamma$-$Fe_2O_3$, and $CoFe_2O_4$ indicate the existence of a nematic-type order of the magnetic particles. Maghemite samples are composed mainly of single particles and Mn samples by bundlelike aggregates of particles. The measured optical anisotropy of these materials could be explained by the shape anisotropy of the particles and the classical light depolarizing factors. The effect of the temperature in these systems could modify the chemical equilibrium between the bulk and the particles surfaces and small-scale aggregations could take place. The potential technological use of nematic ferrofluids could be to make liquid-crystal devices that can be switched by small magnetic fields.

## ACKNOWLEDGMENTS

We thank Dr. F. A. Tourinho and Dr. V. Cabuil, who furnished the ferrofluids, Dr. P. Vachette, and Dr. A. M. Levelut for very helpful discussions of SAXS results. It is also a pleasure to thank M. Robert for important comments and recommendations.

[1] A. R. V. Bertrand, Rev. Inst. Fr. Petr. **25**, 15 (1970).
[2] R. E. Rosensweig, in *Ferrohydrodynamics* (Cambridge University Press, Cambridge, MA, 1985).
[3] R. Anthore, C. Petipas, D. Chandesris, and A. Martinet, J. Phys. (Paris) Colloq. C2, Suppl. **38**, 203 (1977).
[4] R. Anthore, S. Gauthier, A. Martinet, and C. Petipas, IEEE Trans. Magn. **MAG-16**, 197 (1980).
[5] A. Guinier and G. Fournet, *Small Angle Scattering of X-Rays* (Wiley, New York, 1955); A. Guinier, *Theorie et Technique de la Radiocristallographie* (Dunod, Paris, 1956).
[6] R. Massart, C. R. Acad. Sci. Paris **291C**, 1 (1980).
[7] F. Tourinho, R. Franck, R. Massart, and R. Perzynski, Prog. Colloid. Polym. Sci. **79**, 128 (1989).
[8] F. Boué, V. Cabuil, J. C. Bacri, and R. Perzynski, J. Magn. Magn. Mater. (to be published).
[9] P. C. Sholten, IEEE Trans. Magn. **MAG-16**, 221 (1980).
[10] M. F. da Silva, F. A. Tourinho, L. Liebert, and A. M. Figueiredo Neto, J. Magn. Magn. Mater. **122**, 57 (1993).
[11] H. W. Davies and J. P. Llewellyn, J. Phys. D **12**, 311 (1979).
[12] A. Martinet, Rheol. Acta **13**, 260 (1974).
[13] C. F. Hayes, J. Colloid. Interf. Sci. **52**, 239 (1975).
[14] P. C. Scholten, IEEE Trans. Magn. **MAG-16**, 221 (1980).
[15] M. M. Woolfson, *An Introduction to X-Ray Crystallography* (Cambridge University Press, Cambridge, MA, 1978).
[16] J. C. Bacri and R. Perzynski, *Magnetic Fluids and Applications* (Unesco English and Technical Division, Lanham, MD, 1992), Pt. 1-7-2.
[17] J. A. Osborn, Phys. Rev. **67**, 351 (1945).
[18] A. Peterlin and H. A. Stuart, Z. Phys. **112**, 129 (1939); *Hand und Gahrbuch der Chemischen Physik,* edited by A. Euchen and K. L. Wolf (Akademische Verlagsges, Leipzig, 1971), Vol. 8, Pt. 1B.
[19] N. F. Borrelli and J. A. Murphy, J. Appl. Phys. **42**, 1120 (1971).